Immunology
The Journal of cells, molecules, systems and technologies

British Society for immunology

IMMUNOLOGY ORIGINAL ARTICLE

Elimination of GPR146-mediated antiviral function through IRF3/HES1-signalling pathway

Hongjun Huang, Na Zhang, Qingqing Xiong, Ruoyu Chen, Chengfei Zhang, Ning Wang, Li Wang, Hua Ren, Mingyao Liu, Min Qian and Bing Du

Shanghai Key Laboratory of Regulatory Biology, Institute of Biomedical Sciences and School of Life Sciences, East China Normal University, Shanghai, China

doi:10.1111/imm.12752
Received 25 December 2016; revised 23 March 2017; accepted 24 April 2017.
Hongjun Huang and Na Zhang contributed equally to this study.
Correspondence: Bing Du and Min Qian, Institute of Biomedical Sciences and School of Life Sciences, East China Normal University, 500 Dongchuan Road, Shanghai 200241, China.
E-mails: bdu.ecnu@gmail.com and mqian@bio.ecnu.edu.cn
Senior author: Bing Du

Summary

As the most important host defence against viral infection, interferon (IFN) stimulates hundreds of antiviral genes (ISGs) that together establish an 'antiviral state'. However, the antiviral function of most ISGs in viral infection still need further exploration. Here, we demonstrated that the expression of G-protein-coupled receptor 146 (GPR146) is highly increased by both IFN-β and IFN-γ in a signal transducer and activator of transcription 1-dependent signalling pathway. Most importantly, overexpression of GPR146 protects the host cells from vesicular stomatitis virus and Newcastle disease virus infection but not from infection by herpes simplex virus. In contrast, the virus-induced IFN-β production changed little in *Gpr146*-knockout cells. Furthermore, the *Gpr146*-deficient mice showed similar susceptibility to wild-type mice with vesicular stomatitis virus infection. Interestingly, the expression of GPR146 in virus-infected cells was strikingly reduced and can partially explain why the viral infection was little influenced in *Gpr146*-knockout mice. Surprisingly, virus-activated IFN regulatory factor 3 (IRF3) signalling not only induces the expression of IFN but also represses GPR146 expression through HES1 (hairy and enhancer of split-1)-mediated transcriptional activity to establish a dynamic equilibrium between pro-viral and antiviral stages in host cells. Taken together, these data reveal the antiviral role of GPR146 in fighting viral infection although the GPR146-mediated protection is eliminated by IRF3/HES1-signalling, which suggests a potential therapeutic significance of both GPR146 and HES1 signalling in viral infection.

Keywords: GPR146; HES1; IRF3; ISGs; viral infection.

Introduction

After first being described in 1957,[1] the understanding of the cellular mechanisms and clinical use of interferon (IFN) has been a major advance in biomedicine. As a critical mediator of host defence against virus challenges, IFN could interfere with viral infection at different stages and influence both innate and adaptive immune responses. Furthermore, IFN are not only antivirals to both RNA and DNA viruses but are also the prototypic modulators for oncology and show effectiveness in treatment of multiple sclerosis. Interestingly, IFN mainly exert their function in host cells by the induction of hundreds of IFN-stimulated genes (ISGs).[2] Almost 2000 human and mouse ISGs have been identified, most of which remain uncharacterized.[3] Hence, further elucidation of the multitude of ISGs will almost certainly lead to new and more efficacious therapeutics for virus infections.

Abbreviations: BMMs, bone-marrow-derived macrophages; CRISPR, clustered regularly interspaced short palindromic repeats; FBS, fetal bovine serum; GPCRs, G-protein-coupled receptors; HSV-1, herpes simplex virus type 1; IFN, interferon; IRF3, interferon regulatory factor 3; ISGs, interferon-stimulated genes; LPS, lipopolysaccharide; NDV, Newcastle disease virus; PAMP, pathogen-associated molecular pattern; PEMs, peritoneal macrophages; Poly (I:C), polyinosine-polycytidylic acid; PPR, pattern recognition receptor; qPCR, quantitative real-time PCR; qPCR, quantitative real-time PCR; STAT1, signal transducer and activator of transcription 1; VSV, vesicular stomatitis virus

With nearly 1000 members, G-protein-coupled receptors (GPCRs) constitute the largest group of cell surface proteins. Hence, it is not surprising that viruses have evolved ways to exploit these receptors to their advantage. Among them, CXC-chemokine receptor-4 (CXCR4) and CC-chemokine receptor-5 (CCR5) are the most famous cell-fusion co-factors for HIV infection. Meanwhile, more GPCRs have been found involved in the regulation of innate and acquired immune responses, such as free fatty acid receptors,[4] purinergic receptors,[5] adenosine receptors,[6] lysophosphatidic acid receptors,[7] dopamine receptors[8] and bile acid receptors.[9] Hence, the identification of key GPCRs involved in virus infection and related immune responses is clinically important in curing and preventing viral infectious diseases.

GPR146 was first identified when searching in genome databases for orthologues of the Rhodopsin family of human GPCRs in 2005.[10] Then, GPR146 was demonstrated to be part of the C-peptide signalling complex and provided a platform for the elucidation of the C-peptide signalosome.[11] C-peptide and GPR146 have been found to have therapeutic potential in the treatment of diabetes and its complications.[12] Although the immune system plays an important role in metabolic diseases, the role and mechanism of GPR146 in the regulation of immune responses remains unknown. Here, we demonstrated that GPR146 is highly increased by IFN through a signal transducer and activator of transcription 1 (STAT1) -dependent signalling pathway, which can be regarded as an ISG. In addition, overexpression of GPR146 in HEK-293T cells reduced vesicular stomatitis virus (VSV) and Newcastle disease virus (NDV) infection obviously in a dose-dependent manner. Unfortunately, the viral infection barely changed in *Gpr146*-deficient mice because the expression of endogenous GPR146 is almost fully eliminated through IFN regulatory factor 3 (IRF3)/HES1 (hairy and enhancer of split-1)-signalling in virus-activated cells. Our data suggest a potential therapeutic significance of both GPR146 and HES1 signalling in viral infection.

Materials and methods

Mice

Gpr146-knockout mice (C57BL/6) were generated using the clustered regularly interspaced short palindromic repeats (CRISPR)/CRISPR-associated protein 9 (Cas9) system. Details of the procedure have been previously described.[13] Sequences of the CRISPR target sites for mouse *Gpr146* in the genome are 5′-TGCCGGA ACCTGCGCCTG-3′. The CRISPR/Cas9 system caused a random deletion of 148 bases in the genome of mouse *Gpr146*, which silenced expression of *Gpr146*. Sequences for primers used for the identification of mutations are 5′-TCCTCTACACAAGAAAGAGGGG-3′ (forward) and 5′-GTAGTAGTCAAGGCTCAGCAGT-3′ (reverse). *Tlr3*-knockout mice (C57BL/6) breeding pairs were kindly provided by Professor Yuping Lai (East China Normal University). Details of the mice were described previously.[14] All mice were housed and bred in specific pathogen-free rooms. All animal experiments were undertaken in accordance with the National Institutes of Health Guide for the Care and Use of Animals and were approved by the East China Normal University Centre for Animal Research.

Chemicals and reagents

Dulbecco's modified Eagle's medium, RPMI-1640, penicillin-streptomycin and Lipofectamine 2000 were purchased from Invitrogen Life Technologies (Carlsbad, CA). Fetal bovine serum (FBS) was purchased from HyClone (Logan, UT). TRIzol reagent, SYBR Premix Ex Taq and PrimeScript RT Master Mix were acquired from Takara (Shiga, Japan). Polyinosine-polycytidylic acid [Poly (I:C)] was obtained from Invivogen (San Diego, CA) and lipopolysaccharide (LPS) from Sigma (St Louis, MO). Recombinant mouse IFN-β and IFN-γ were obtained from Sino Biological (Beijing, China) and PROSPEC (Ness-Ziona, Israel), respectively. The STAT1 inhibitor (fludarabine, 100 μg/ml) was purchased from Calbiochem (San Diego, CA). Dual-Luciferase Reporter assay reagent was purchased from Promega (Madison, WI). Antibodies specific to IRF3 and phosphorylated IRF3 were obtained from Cell Signaling Technology (Danvers, MA). Polyclonal anti-GAPDH antibody was obtained from Biogot technology (Nanjing, China). Antibodies specific to CD11b and F4/80 for FACS were purchased from BD Biosciences (Franklin Lakes, NJ).

Cell culture and isolation

RAW264.7, Vero and HEK-293T cells were purchased from the American Type Culture Collection (Manassas, VA). For cell culture, RAW264.7, Vero and HEK-293T cells were maintained in complete Dulbecco's modified Eagle's medium (supplemented with 10% FBS and penicillin-streptomycin). Peritoneal macrophages (PEMs) were harvested from mice after thioglycollate medium injection. Briefly, mice were injected with 3% sterile thioglycollate medium intraperitoneally (3 ml per mouse). Four days later, the mice were killed, and RPMI-1640 medium was injected intraperitoneally and then retrieved. The cells were then treated with red blood cell lysis buffer and washed with PBS. The PEMs were cultured in complete RPMI-1640 medium containing 10% FBS and penicillin-streptomycin for related experiments. Bone-marrow-derived macrophages (BMMs) were isolated and cultured as previously described.[15] The

generated PEMs and BMMs were $CD11b^+$ and $F4/80^+$ (purity > 90%).[16]

Virus collection and infection

Herpes simplex virus type 1 (HSV-1) and Indiana serotype of VSV were gifts from Professor Ping Wang (Tongji University). NDV-GFP virus was kindly provided by Professor Jiahuai Han (Xiamen University). VSV-GFP virus was a gift from Dr Andrea Cimarelli (Ecole Normale Supérieure de Lyon). These viruses were propagated in a monolayer of Vero cells, and the titres were determined by plaque assays. Cells were infected with viruses for the indicated time and dose. For *in vivo* survival studies, age- and sex-matched mice were intraperitoneally infected with VSV (1×10^8 plaque-forming units/g). For *in vivo* studies of VSV replication, age- and sex-matched mice were intraperitoneally infected with VSV (1×10^8 plaque-forming units per mouse) for 24 hr.

Plasmids and transfection

GPR146 plasmid was obtained from GeneCopoeia, Inc. (Rockville, MD) *IFN-β*-luciferase, renilla, and *TBK1* were kindly provided by Professor Ping Wang (Tongji University). Transfections were performed using calcium phosphate-DNA co-precipitation for HEK-293T cells according to the manufacturer's instructions. The cells transfected with the same amount of empty vector (Emv) was used as control.

RNA interference

Peritoneal macrophages were seeded into 12-well plates at 1×10^6 cells per well overnight and transfected with 50 nmol small interfering RNA (siRNA) duplexes using Lipofectamine 2000, according to the manufacturer's instructions. The cells transfected with the same amount of universal non-targeting siRNAs were used as negative control (si NC). The target sequences for the mouse *Irf3* siRNAs were *Irf3*-A 5′-ACAAUAGCAAGGACCCUUAUGACCC-3′, *Irf3*-B 5′-GGAACAAUGGGAGUUCGAGGUGACC-3′ and *Irf3*-C 5′-CGGAGGCUUAGCUGACAAAGAAGGG-3′.The target sequence for the mouse *Stat1* siRNA was 5′-GGAA AAGCAAGCGUAAUCUTT-3′.[17] The target sequence for the mouse *Hes1* siRNA was 5′-CGACACCGGACAAACC AAA-3′.[18]

Real-time quantitative PCR

Total RNA was isolated from HEK-293T, primary macrophages and RAW264.7 cells using TRIzol reagent (Takara) according to the manufacturer's instructions and subjected to reverse transcription with PrimeScript RT Master Mix Perfect Real Time Kit (Takara). Five hundred nanograms of cDNA was used as a template and subjected to quantitative PCR (qPCR) using universal SYBR Green PCR Master Mix (Takara). Primers for each cytokine and gene are described in the Supplementary material (Table S1).

Western blots

After VSV stimulation, PEMs were washed twice with cold PBS and lysed by RIPA buffer containing protease inhibitors. The protein concentration was measured by BCA assay (Pierce, Rockford, IL) and equalized to the same concentration with the extraction reagent. Samples were loaded and heated for 15 min at 100°, separated by 10% SDS–PAGE, transferred to nitrocellulose membranes, and blocked with 5% bovine serum albumin. Following incubation with primary antibodies and incubation with the appropriate fluorescent secondary antibodies, the immunoreactive bands were visualized by the Odyssey laser digital imaging system (Gene Company Limited, Hong Kong China).

Luciferase reporter assays

Transfected cells were lysed and assayed for luciferase activity using the Luciferase Assay Kit, according to the manufacturer's protocol (Promega). The data were normalized for transfection efficiency by comparing firefly luciferase activity with that of renilla luciferase.

Viral plaque assays

The VSV plaque assays were performed on Vero cells in 12-well culture plates at 2×10^5 cells per well and allowed to grow overnight. Supernatant from VSV-infected cells were serially diluted and infected in Vero cells for 1 hr. The cells were then covered with growth medium containing 1·5% (mass/volume) low-melting-point agarose. Plaques were counted after 16 hr.

Lung histology

Lungs from control or virus-infected mice were dissected, fixed in 4% paraformaldehyde, embedded into paraffin, cut into sections, stained with haematoxylin & eosin solution, and examined by light microscopy for histological changes.

Flow cytometry

Peritoneal macrophages were infected with VSV-GFP (0·01 MOI) for 12 hr, and VSV-GFP was measured by FACS. Mature BMMs were determined by CD11b and F4/80 double staining using a flow cytometer (all from BD Biosciences). The data were analysed with FLOWJO software (FlowJo, LLC, Ashland, OR).

Statistical analysis

Kaplan–Meier curves present mouse survival rates; all statistical analyses were performed with PRISM 5.0 (GraphPad Software, Inc., La Jolla, CA). The data are expressed as the mean ± SD by a Student's *t*-test. For *in vivo* experiments, values are expressed as the mean ± SEM of *n* animals. Statistical values achieving $P < 0{\cdot}05$ were considered to be statistically significant.

Results

The expression of GPR146 is increased significantly by IFN

To explore the potential role of GPCRs in IFN-mediated immune regulation, we examined the expression of different GPCRs in IFN-treated macrophages. As shown in Fig. 1(a–c), the expression of *Gpr146* in PEMs, the macrophage-like cell line RAW264.7 cells and BMMs were all enhanced by both IFN-β and IFN-γ. Accordingly, we also observed a consensus sequence for STAT1 binding on the promoter of mouse *Gpr146* (Fig. 1d), implying that GPR146 is regulated by STAT1-associated signalling. Similar observations were also found on the promoter of human *GPR146* (see Supplementary material, Fig. S1a). Therefore, we knocked down the expression of *Stat1* in PEMs (Fig. 1e) and found that IFN-induced induction of *Gpr146* transcription was significantly reduced. (Fig. 1f). Furthermore, we also treated the PEMs with STAT1 inhibitor (fludarabine, 100 μg/ml). The ubiquitin-like protein ISG15 is a critical IFN-induced antiviral molecule that protects against several viral infections.[19] Indeed, the IFN-enhanced expression of *Isg15* was strikingly impaired by

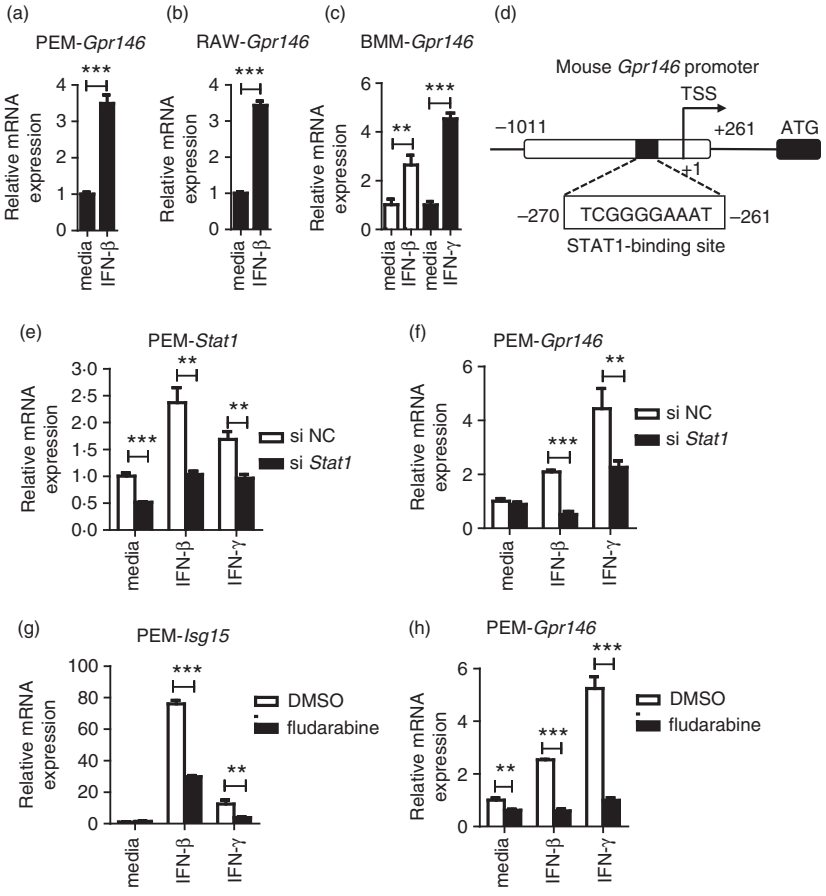

Figure 1. GPR146 is an interferon-stimulated gene (ISG). (a, b) Quantitative PCR analysis of *Gpr146* expression in primary peritoneal macrophages (PEMs) (a), RAW264.7 cells (b) stimulated with interferon-β (IFN-β) (100 ng/ml) for 2 hr. (c) Quantitative PCR analysis of *Gpr146* expression in bone-marrow-derived macrophages (BMMs) stimulated with IFN-β (100 ng/ml) or IFN-γ (100 ng/ml) for 2 hr. (d) The potential signal transducer and activator of transcription 1 (STAT1) -binding sites in the promoter of mouse *Gpr146* were predicted by ALGGEN-PROMO. (e, f) Quantitative PCR analysis of *Stat1* (e) and *Gpr146* (F) expression in PEMs transfected with *Stat1* siRNA and then stimulated with IFN-β (100 ng/ml) or IFN-γ (100 ng/ml) for 2 hr. (g) Quantitative PCR analysis of *Isg15* expression in PEMs pretreated for 30 min with the STAT1 inhibitor (fludarabine, 100 μg/ml) and then stimulated with IFN-β (100 ng/ml) or IFN-γ (100 ng/ml) for 2 hr. (h) Quantitative PCR analysis of *Gpr146* expression in PEMs treated as in (g). *Gpr146* expression was normalized to that of the *Gapdh* internal control in each sample. The data are shown as the mean ± SD. $^{**}P < 0{\cdot}01$; $^{***}P < 0{\cdot}001$. All experiments were performed two or three times with similar results.

fludarabine, suggesting that the STAT1 inhibitor was working properly (Fig. 1g). Meanwhile, we found that IFN-induced induction of *Gpr146* transcription was also significantly impaired by fludarabine (Fig. 1h). Taken together, our data suggest that GPR146 could be recognized as an ISG.

GPR146 selectively inhibits RNA virus propagation

To elucidate the potential role of GPR146 in virus infection, we overexpressed the *GPR146* in HEK-293T cells (Fig. 2a). Our data showed that the overexpression of *GPR146* increased the viability of HEK-293T cells in a dose-dependent manner in VSV infection (Fig. 2b). Meanwhile, the RNA level of VSV was also decreased in *GPR146*-overexpressing cells (Fig. 2c). Furthermore, a similar restriction of the virus titre was observed by *GPR146* in a plaque assay (Fig. 2d). This type of inhibition of VSV replication by *GPR146* could be found in different titres (Fig. 2e) and times (Fig. 2f) during infection. At the same time, we infected *GPR146*-overexpressing cells with NDV and *GPR146* reduced NDV replication (Fig. 2g). HSV-1 is commonly used as a DNA virus model. Analysis of the expression of the HSV-1 DNA polymerase gene (UL-30) represents an indication of viral replication.[20] In contrast, the infection of HSV-1 was only slightly changed by *GPR146* (Fig. 2h,i), suggesting that the GPR146-mediated inhibition of virus infection is limited to RNA virus. On the whole, GPR146 plays a protective role in infected cells through specifically reducing RNA virus but not DNA virus propagation.

The expression of type I IFN is little changed by GPR146

As a member of ISGs, GPR146 has been shown to have great potential in protecting cells from RNA virus infection. Hence, we constructed *Gpr146* knockout mice (see Supplementary material, Fig. S1b–e) to better understand the GPR146-mediated antiviral function. As type I IFN are important for host defence against viruses,[21] we detected the expression of type I IFN in *Gpr146* knockout cells to investigate whether GPR146 influences production of IFN. As shown in Fig. 3(a), the mRNA expression level of *Ifn-β* changed little in *Gpr146* knockout PEMs. As a well-recognized synthetic analogue of double-stranded RNA, Poly (I:C) is commonly used to mimic RNA virus infection and activate the extracellular Toll-like receptor 3 (TLR3) -associated or the intracellular RIG-I (Retinoic acid-inducible gene I)-associated signalling pathway.[22–24] Hence, the PEMs were treated by Poly (I:C) with or without Lipofectamine 2000 (Fig. 3b) to mimic the RNA virus infection, but no significant influence on *Ifn-β* production was observed in the *Gpr146* knockout cells. Similar data were found in *Gpr146* knockout BMMs (Fig. 3c). Compared with the wild-type BMMs, the induction of the *Ifn-α4*, which is an IRF3-responsive gene,[25] was little changed in $Gpr146^{-/-}$ BMMs in response to Poly (I:C) transfection (Fig. 3d). Consequently, the phosphorylation of IRF3, which is the key transcription factor of IFN-*β*, was influenced little in *Gpr146* knockout cells during viral infection (Fig. 3e). Furthermore, *GPR146* and *TBK1* were both overexpressed in HEK-293T cells to appraise the influence on the transcriptional activity of the *IFN-β* promoter region. TBK1 is an essential component of the IRF3 signalling pathway, which phosphorylates IRF3 and induces IFN-*β* production.[26] Although the transcriptional activity of *IFN-β* core promoter was increased by *TBK1*, little was changed in *GPR146*-transfected cells (Fig. 3f). In the meantime, the supernatants from *TBK1*- and *GPR146*-overexpressing cells were collected to detect the protective role of released IFN. Consequently, the supernatant of *TBK1*-expressing cells reduced both VSV and NDV replication. However, the RNA virus infection was barely influenced in the supernatant of *GPR146*-expressing cells (Fig. 3g,h). Therefore, these data suggest that the expression of IFN-*β* is little changed by GPR146.

Gpr146-deficient mice have similar susceptibility to VSV infection compared with wild-type mice

To investigate the role of GPR146 in protecting mice from VSV infection, we challenged age- and sex-matched $Gpr146^{+/+}$ and $Gpr146^{-/-}$ mice with VSV intraperitoneally. However, the survival of VSV infection had little difference between wild-type and *Gpr146* knockout mice (Fig. 4a). The distributions of VSV in liver, spleen and lung were all slightly influenced in *Gpr146*-deficient mice (Fig. 4b). Accordingly, the virus-induced lung tissue injury was almost the same in wild-type and *Gpr146* knockout mice (Fig. 4c). The VSV replication in PEMs was slightly influenced by *Gpr146* knockout, as verified with different titres (Fig. 4d) and at different times (Fig. 4e). Similar data were also observed in *Gpr146* knockout BMMs (Fig. 4f). Furthermore, if we infected the PEMs with VSV-GFP for 12 hr, the infection efficiency was little changed in *Gpr146* knockout PEMs (Fig. 4g). In conclusion, although overexpression of GPR146 in host cells showed significant antiviral function in fighting against RNA virus infection, *Gpr146* knockout mice demonstrated similar susceptibility to VSV infection both in primary macrophages and in a mouse model, implying that the expression of endogenous GPR146 may be decreased during viral infection.

The expression of GPR146 is down-regulated by pathogens

To illustrate the regulation of endogenous GPR146 in virus infection, we checked the expression of GPR146 in

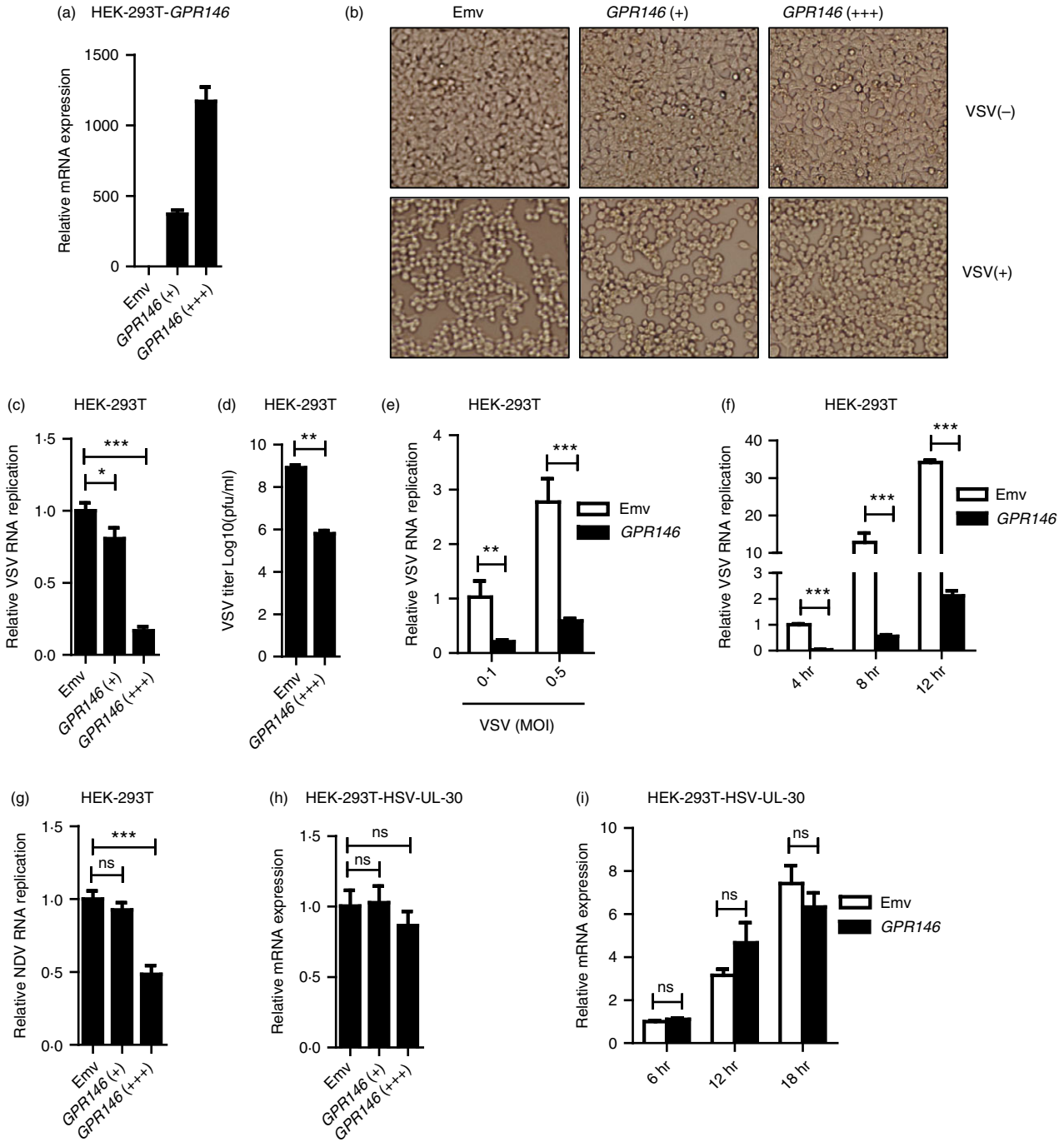

Figure 2. GPR146 selectively inhibits RNA virus propagation. (a) Quantitative PCR analysis of *GPR146* expression in HEK-293T cells transfected for 28 hr with different amounts (0·6 and 1·8 μg) of *GPR146* plasmid. (b) HEK-293T cells transfected with *GPR146* plasmid as described in (a) were infected with vesicular stomatitis virus (VSV) (0·1 MOI) for 9 hr and then observed under a microscope. Original magnification 10×. (c) Quantitative PCR analysis of VSV RNA replicates in (b). (d) VSV titres were measured in (b) by standard plaque assay. (e, f) Quantitative PCR analysis of VSV RNA replicates in *GPR146*-overexpressing (1·8 μg) HEK-293T cells infected by VSV with the indicated MOI (e) and times (f). (g) Quantitative PCR analysis of Newcastle disease virus (NDV) RNA replicates in HEK-293T cells transfected with *GPR146* plasmid as described in (a) and infected with NDV (0·25 MOI) for 12 hr. (h) Quantitative PCR analysis of herpes simplex virus (HSV) UL-30 expression in HEK-293T cells transfected with *GPR146* plasmid as described in (a) and infected with HSV-1 (0·5 MOI) for 18 hr. (i) Quantitative PCR analysis of HSV-UL-30 expression in *GPR146*-overexpressing (1·8 μg) HEK-293T cells infected for the indicated times with HSV-1 (0·5 MOI). *GAPDH* was used as an internal control for quantitative PCR. The data are shown as the mean ± SD. $*P < 0{\cdot}05$; $**P < 0{\cdot}01$; $***P < 0{\cdot}001$; ns, not significant. All experiments were performed three times with similar results. [Colour figure can be viewed at wileyonlinelibrary.com]

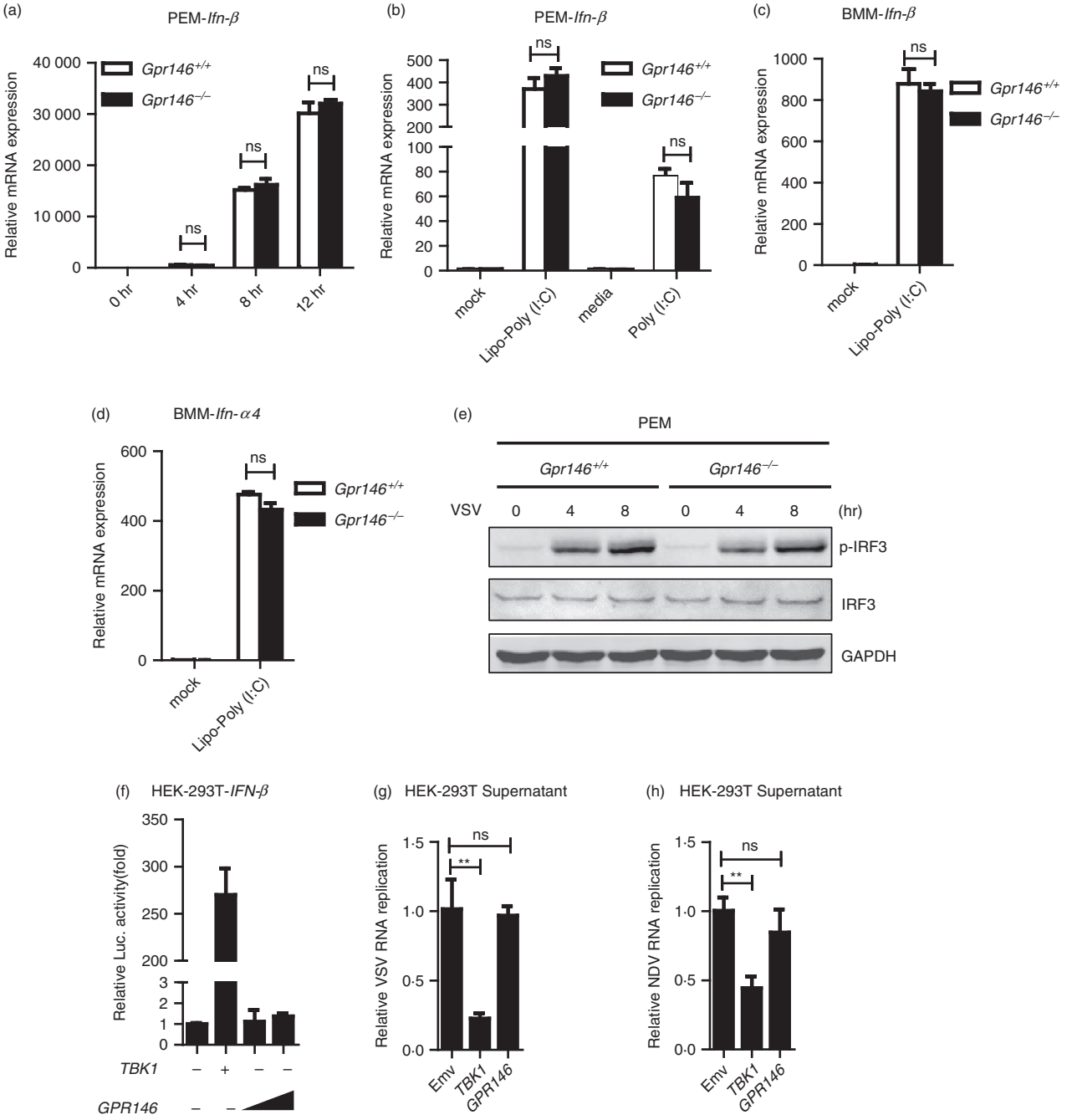

Figure 3. The expression of type I interferon (IFN) is little changed by GPR146. (a) Quantitative PCR analysis of *Ifn-β* expression in $Gpr146^{+/+}$- and $Gpr146^{-/-}$ peritoneal macrophages (PEMs) infected with vesicular stomatitis virus (VSV) (1·0 MOI) for the indicated times. (b) Quantitative PCR analysis of *Ifn-β* expression in $Gpr146^{+/+}$ and $Gpr146^{-/-}$ PEMs transfected with Poly (I:C) (1·0 μg/ml) or stimulated with Poly (I:C) (10 μg/ml) for 4 hr. (c, d) Quantitative PCR analysis of *Ifn-β* (c) and *Ifn-α4* (d) expression in $Gpr146^{+/+}$-and $Gpr146^{-/-}$ bone-marrow-derived macrophages (BMMs) transfected with Poly (I:C) (1·0 μg/ml) for 4 hr. (e) Immunoblot analysis of phosphorylated IRF3 and total IRF3 in lysates of $Gpr146^{+/+}$ and $Gpr146^{-/-}$ PEMs infected for the indicated times with VSV (1·0 MOI). (f) *IFN-β* promoter activity in *TBK1*- and *GPR146*-transfected HEK-293T cells detected by luciferase reporter assay. (g, h) Conditioned-media from HEK-293T cells transfected with the indicated plasmids for 28 hr were used to treat freshly plated HEK-293T cells. The cells were infected with VSV (0·1 MOI) or Newcastle disease virus (NDV) (0·25 MOI) for 9 hr after conditioned-media treatment, and VSV RNA replicates (g) or NDV RNA replicates (h) were detected by quantitative PCR. *Gapdh* was used as an internal control for quantitative PCR. The data are shown as the mean ± SD. $^{**}P < 0{\cdot}01$; ns, not significant. All experiments were performed three times with similar results.

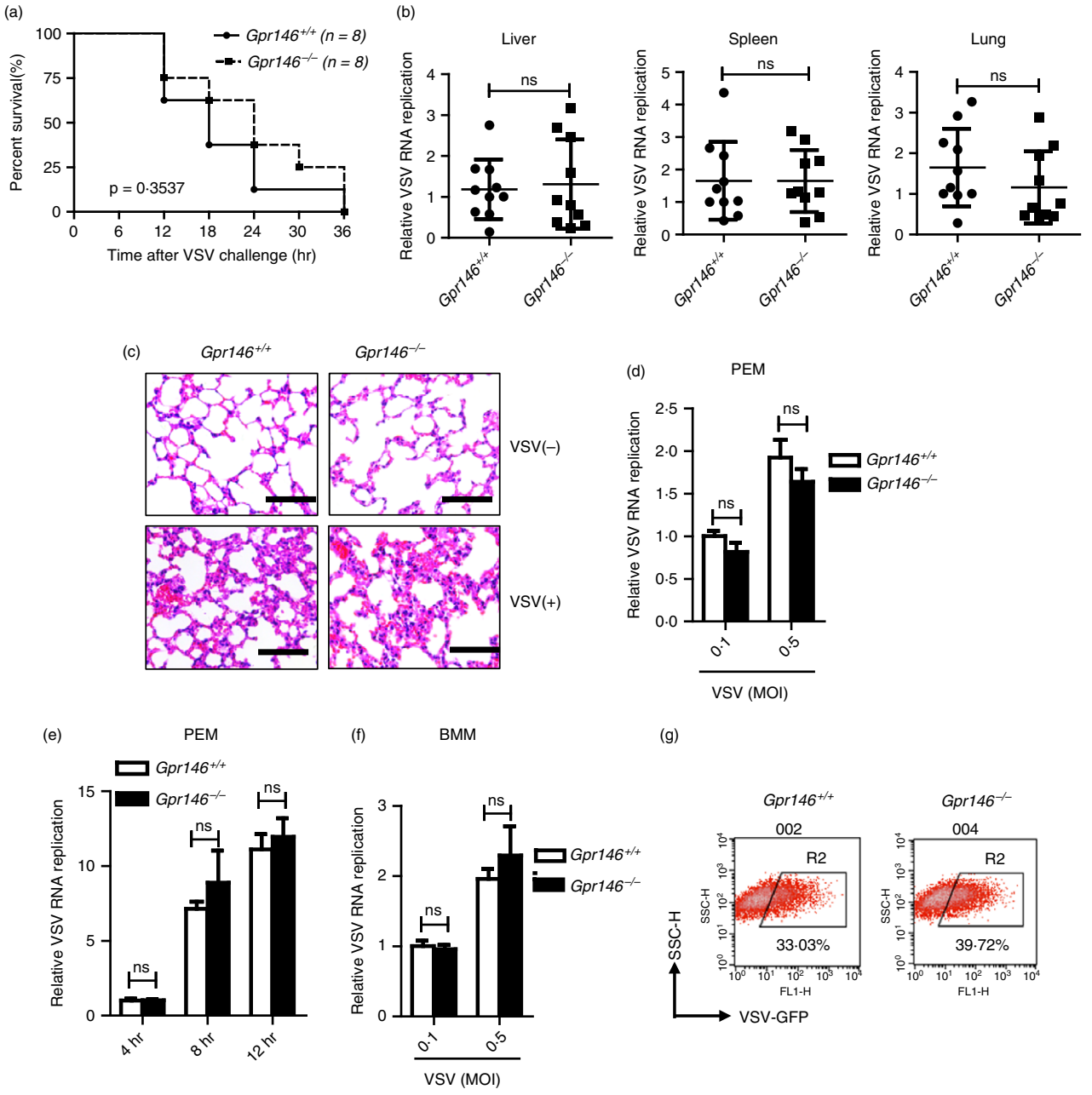

Figure 4. Similarity of viral infection in wild-type and *Gpr146*-knockout mice. (a) Survival of 8-week-old $Gpr146^{+/+}$ and $Gpr146^{-/-}$ mice given intraperitoneal injections of vesicular stomatitis virus (VSV) (1×10^8 pfu/g) ($n = 8$ per group). (b) Determination of VSV loads in organs by quantitative PCR from $Gpr146^{+/+}$ and $Gpr146^{-/-}$ mice infected with VSV (1×10^8 pfu per mouse) intraperitoneally for 24 hr ($n = 10$ per group). (c) Haematoxylin & eosin staining of lung sections from mice in (b). Scale bar, 200 μm. (d, e) Quantitative PCR analysis of VSV RNA levels from $Gpr146^{+/+}$ and $Gpr146^{-/-}$ peritoneal macrophages (PEMs) infected with the indicated VSV MOI (d) and for the indicated times (e). (f) Quantitative PCR analysis of VSV RNA levels from $Gpr146^{+/+}$ and $Gpr146^{-/-}$ bone-marrow-derived macrophages (BMMs) infected with the indicated VSV MOI for 12 hr. (g) PEMs from $Gpr146^{+/+}$ and $Gpr146^{-/-}$ mice were infected VSV-GFP (0·01 MOI) for 12 hr, and VSV-GFP was measured by FACS. *Gapdh* was used as an internal control for quantitative PCR. The data are shown as the mean ± SD. ns, not significant. All experiments were performed two or three times with similar results. [Colour figure can be viewed at wileyonlinelibrary.com]

virus-infected cells. As shown in Fig. 5(a,b), the expression of *Gpr146* in PEMs was strikingly eliminated in a time- and dose-dependent manner by VSV. Similar data were also observed in RAW264.7 cells (Fig. 5c). Meanwhile, the expression of *Gpr146* could be reduced dramatically by HSV-1 in a time-dependent manner (Fig. 5d). In addition, *GPR146* expression in the liver of hepatitis B virus-infected patients is significantly

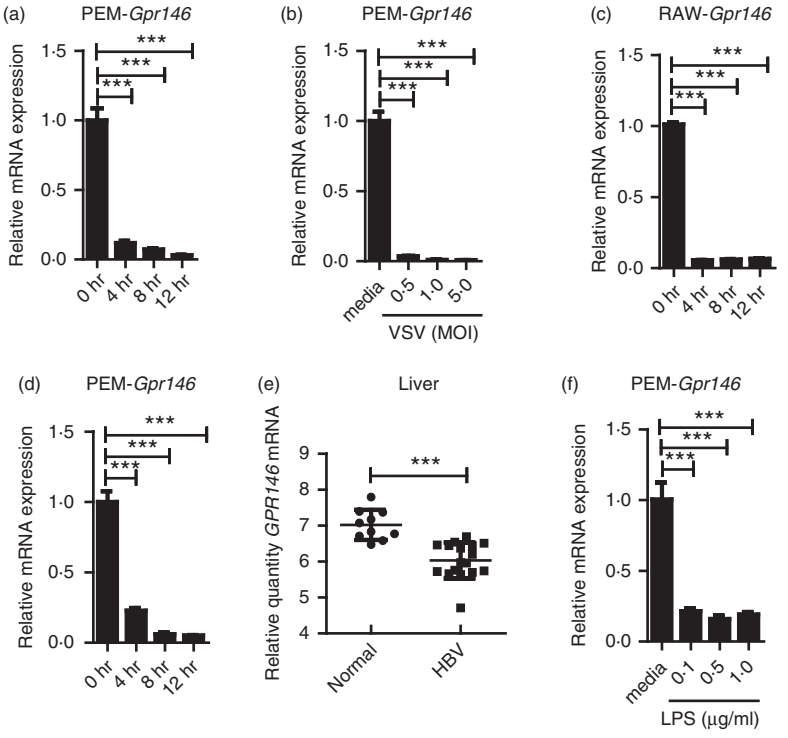

(g)

VSV (1 MOI)	0 hr	4 hr	8 hr	12 hr
Ct (cycles)	25·64	28·01	31·12	32·13
Gpr146	25·54	27·76	31·30	32·18
	25·79	27·63	31·51	32·11

Figure 5. GPR146 is down-regulated by pathogens. (a) Quantitative PCR analysis of *Gpr146* expression in peritoneal macrophages (PEMs) infected with vesicular stomatitis virus (VSV) (1·0 MOI) for the indicated times. (b) Quantitative PCR analysis of *Gpr146* expression in PEMs infected with the indicated VSV MOI for 8 hr. (c) Quantitative PCR analysis of *Gpr146* expression in RAW264.7 cells infected with VSV (1·0 MOI) for the indicated times. (d) Quantitative PCR analysis of *Gpr146* expression in PEMs infected with herpes simplex virus type 1 (HSV-1) (1·0 MOI) for the indicated times. (e) *GPR146* expression is analysed in human livers infected with hepatitis B virus (HBV) from GEO Profiles. (f) Quantitative PCR analysis of *Gpr146* expression in PEMs stimulated with the indicated amounts (ng/ml) of lipopolysaccharide (LPS) for 4 hr. (g) Amplifying cycles of *Gpr146* expression in (a). *Gapdh* was used as an internal control for quantitative PCR. The data are shown as the mean ± SD. ***$P < 0{\cdot}001$. All experiments were performed three times with similar results.

decreased (Fig. 5e). Interestingly, the expression of *Gpr146* was robustly reduced by LPS (Fig. 5f), suggesting that GPR146 may be regulated in a TLR-dependent manner. The expression of GPR146 is significantly reduced by RNA virus (VSV), DNA virus (HSV-1), and the component of Gram-negative bacteria (LPS), these pathogens activate a sharing signalling pathway in innate immune response through pattern recognition receptors (PRRs),[27]suggesting that GPR146 may be negatively regulated by a common signalling pathway of PRRs. To fully understand the effect of VSV on *Gpr146* expression level, qPCR analysis was performed, and when PEMs were VSV infected, for 4–12 hr, the amplifying cycles increased from 25 to 32, indicating a decrease in *Gpr146* expression (Fig. 5g). Taken together, these data demonstrated that GPR146 plays a protective role in RNA virus infection, and the expression of GPR146 is dramatically reduced by these pathogens. This phenomenon could partially explain why the *Gpr146* knockout mice showed a susceptibility to VSV infection similar to that of wild-type mice.

Elimination of GPR146-mediated antiviral function through IRF3/HES1-signalling pathway

Since the regulation of GPR146 may be in a common signalling pathway of PRRs, we treated PEMs with Poly (I:C), in the presence or absence of Lipofectamine 2000 to mimic the RNA virus infection and found that the expression of *Gpr146* was reduced (Fig. 6a), which suggested that the TLR3- or RIG-I-associated signalling is

involved in the suppression of GPR146. Meanwhile, we treated *Tlr3*$^{+/+}$ and *Tlr3*$^{-/-}$ PEMs with both Poly (I:C) and LPS, the expression of *Gpr146* was significantly reduced by Poly (I:C) and LPS in *Tlr3*$^{+/+}$ PEMs. Whereas, the expression of *Gpr146* was little decreased by Poly (I:C) in *Tlr3*$^{-/-}$ PEMs (see Supplementary material, Fig. S1f,g). Collectively, these data suggested that the TLR-mediated signalling pathway plays the key role in regulation of GPR146 expression. Additionally, previous work reported that an IRF3-dependent but type I IFN-independent pathway strongly inhibits the expression of retinoid X receptor α (RXRα) through induction of the transcription suppressor HES1.[28] Considering the previous observation, we determined whether the expression of GPR146 was down-regulated by this signalling pathway. As shown in Fig. 6(b,c), the Poly (I:C)-reduced *Gpr146* expression was rescued in *Irf3*-knockdown PEMs. Consequently, a series of consensus sequences for HES1 binding sites on the promoter of mouse *Gpr146* were found by bioinformatics analysis (Fig. 6d). Similar observations were also found on the promoter of human *GPR146* (see Supplementary material, Fig. S1a). The knockdown of *Irf3* in PEMs decreased the expression of *Hes1* (Fig. 6e), which also suggested that HES1 is positively regulated by IRF3 and is consistent with the previous work. Interestingly, HES1 has already been found as a homeostatic suppressor of inflammatory responses that exerts its suppressive function by regulating transcription elongation.[29] To further confirm the negative regulation of GPR146 by the IRF3/HES1-signalling pathway, we silenced the expression of *Hes1* in PEMs (Fig. 6f). Therefore, we checked the expression of *Gpr146* in *Hes1*-silenced PEMs and found that the Poly (I:C)-reduced *Gpr146* expression was almost totally rescued in *Hes1* knockdown cells (Fig. 6g) and suggested the dominant role of HES1 in negative regulation of GPR146. Accordingly, the *Gpr146*-mediated virus inhibition was also rescued in *Gpr146*$^{+/+}$ PEMs when we silenced the expression of *Hes1*, however, the VSV RNA replication was little changed by *Hes1* knockdown in *Gpr146*$^{-/-}$ PEMs (Fig. 6h). When we knocked down the expression of *Hes1* in wild-type and *Gpr146* knockout PEMs, *Gpr146*-mediated antiviral function was aroused during VSV infection (Fig. 6i). Similar data were observed in VSV-GFP infection (Fig. 6j). In conclusion, our data demonstrated that HES1 could be a negative regulator in virus infection through eliminating the interferon-stimulated protein GPR146-mediated antiviral function (Fig. 7).

Discussion

Considering the limited viral components produced by viruses, as well as the high mutation of viral genomes to develop drug resistance, recent antiviral drug development strategies have focused on targeting host proteins that are essential for viral replication.[30] As the largest class of cell-surface receptors, GPCRs are encoded by > 1000 genes in the human genome. It has been estimated that 50% of all modern drugs and almost one-quarter of the top 200 best-selling drugs modulate GPCR activity.[31] Additionally, there is growing evidence that GPCRs are involved in virus infection.[32] Hence, we conducted a systematic analysis to identify and validate the IFN-stimulated GPCRs associated with virus infection. After screening dozens of GPCRs stimulated by IFN, we identified GPR146 as an antiviral factor specific to RNA virus infection, which has great potential as an antiviral drug target. We found that the expression of GPR146 was almost totally eliminated during virus infection through the IRF3/HES1-signalling pathway, which could be considered an escape mechanism of the virus from host defences. Therefore, when we knocked down expression of HES1 in wild-type and *Gpr146* knockout mice, the protective role of GPR146 in viral infection was aroused and suggested that the HES1 could be a negative regulator in GPR146-mediated host defences against viral infection.

As a typical ISG, GPR146 can be dramatically increased by IFN in a STAT1-dependent manner. The overexpression of GPR146 reduced RNA virus infection in a dose-dependent manner, suggesting that GPR146 could be a very important antiviral mediator in protecting host cells from infection. This type of protection is independent of IFN-associated innate immune responses. Hence, it would be easy to assume that the invading virus induced the release of IFN and then increase the expression of GPR146, which reduced the replication of the RNA virus

Figure 6. GPR146 expression is regulated through the antiviral IRF3/HES1-signalling pathway. (a) Quantitative PCR analysis of *Gpr146* expression in peritoneal macrophages (PEMs) transfected with Poly (I:C) (1·0 μg/ml) or stimulated with Poly (I:C) (10 μg/ml) for 4 hr. (b) Quantitative PCR analysis of *Irf3* expression in PEMs transfected with *Irf3* siRNA. (c) Quantitative PCR analysis of *Gpr146* expression in PEMs transfected with *Irf3* siRNA and then transfected with Poly (I:C) (1·0 μg/ml) or stimulated with Poly (I:C) (10 μg/ml) for 4 hr. (d) The potential HES1 binding sites in the promoter of mouse *Gpr146* were predicted by ALGGEN-PROMO. (e) Quantitative PCR analysis of *Hes1* expression in (c). (f) Quantitative PCR analysis of *Hes1* expression in PEMs transfected with *Hes1* siRNA. (g) Quantitative PCR analysis of *Gpr146* expression in PEMs transfected with *Hes1* siRNA and then transfected with Poly (I:C) (1·0 μg/ml) or stimulated with Poly (I:C) (10 μg/ml) for 4 hr. (h, i) Quantitative PCR analysis of vesicular stomatitis virus (VSV) RNA replicates in *Gpr146*$^{+/+}$ and *Gpr146*$^{-/-}$ PEMs transfected with *Hes1* siRNA and then infected for the indicated times with VSV (0·5 MOI). (j) *Gpr146*$^{+/+}$ and *Gpr146*$^{-/-}$ PEMs transfected with *Hes1* siRNA were infected with VSV-GFP (0·01 MOI) for 12 hr, and VSV-GFP was measured by FACS. *Gapdh* was used as an internal control for quantitative PCR. The data are shown as the mean ± SD. *$P < 0·05$; **$P < 0·01$; ***$P < 0·001$. All experiments were performed two or three times with similar results. [Colour figure can be viewed at wileyonlinelibrary.com]

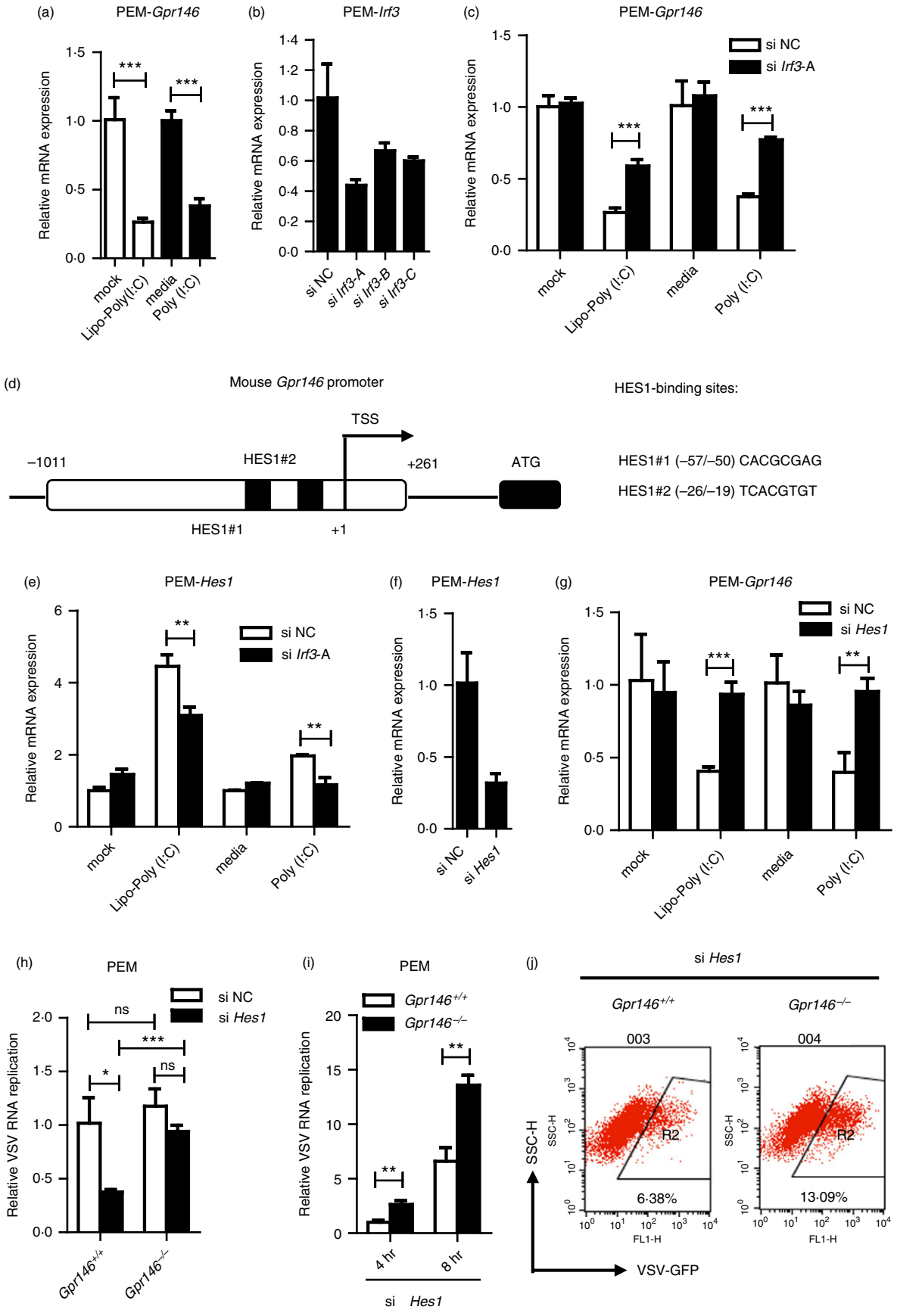

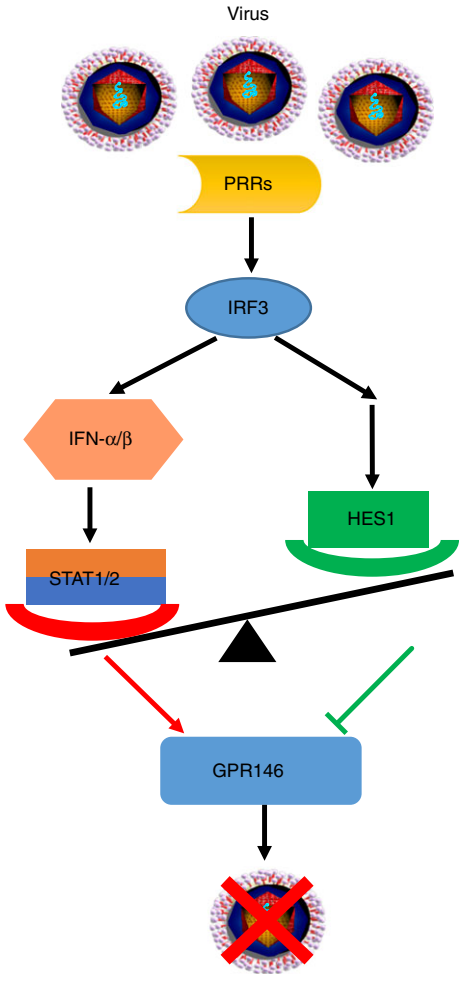

Figure 7. The model of viruses escape from GPR146-mediated antiviral function. As an interferon-stimulated gene, GPR146 selectively inhibits RNA virus propagation. However, activation of IRF3 through pattern recognition receptors (PRRs) results in the reduction of GPR146 through HES1. The repression of GPR146 by viruses eliminates the interferon-stimulated protein GPR146-mediated antiviral function. [Colour figure can be viewed at wileyonlinelibrary.com]

in the infected cells. To our surprise, when we infected wild-type and *Gpr146*-mutated mice, the survival and resident viruses in different tissues were similar. For this reason, we checked the expression of GPR146 in viral infection and found that the expression of GPR146 was reduced to almost non-detectable levels. Our result implied that the invading virus not only activated innate immune responses but also took advantage of the host components to escape from the immune surveillance.

Meanwhile, the expression of GPR146 was not only inhibited by the virus but also inhibited by LPS, which is a commonly used pathogen-associated molecular pattern (PAMP) to activate TLR4-associated signalling. The recognition of PAMPs by PRRs is the initiation of innate and adaptive immunity against pathogens and is involved in autoimmune, chronic inflammatory and infectious diseases.[33] Although a series of PRRs that include TLRs, RIG-I-like receptors, NOD-like receptors and C-type lectin receptors have been clarified by function or by localization, the intracellular signalling cascades triggered by these PRRs have similar and shared signaling components.[34] Among them, the activation of IRF3 is essential in viral infection as well as bacterial infection, suggesting the potential role of IRF3 in these processes. Surprisingly, silencing of IRF3 in PEMs significantly recovered the Poly (I:C)-induced decrease of GPR146 expression and implies the potential of GPR146 in an IRF3-mediated immune response.

As the 'key regulators' of innate antiviral immunity, IRF3 and IRF7 play very important roles in IFN production.[35] Upon stimulation of host cells by invading virus, IRF3 is activated by TBK1-mediated phosphorylation through dimerization and nuclear translocation, which lead to induce IFN-β expression.[36] Then, the released IFN-β leads to induction of hundreds of ISGs, recruitment and activation of immune cells through activating the Janus kinase/STAT pathway.[37] Therefore, the activation of the IRF3 signalling pathway is thought to be the key step in antiviral immune responses. We found that IRF3 is not only upstream of IFN, but also activates HES1, which has been identified as a negative regulator to innate and acquired immune responses.[29,38] HES1 is a transcription factor that is regulated by the NOTCH-, HEDGEHOG- and WNT-signalling pathways. Aberrant expression of these pathways is a common feature of cancer cells.[39] Furthermore, the released IFN could activate IFN receptors to induce STAT1, which is an important positive regulator to most ISGs, such as ISG20 and GPR146. Accordingly, we also observed a conserved STAT1-binding site in the promoter of *GPR146*, which is consistent with the increasing of GPR146 expression by IFN, suggesting that GPR146 could be regarded as an ISG. Unfortunately, massive HES1 binding sites were also localized in the promoter of *GPR146*, which eliminates GPR146 expression during virus infection by activating IRF3 signalling. The regulation of IFN and GPR146 by IRF3-associated signalling establishes a dynamic equilibrium between pro-viral and antiviral stages in host cells. Taken together, these data reveal the antiviral role of GPR146 in fighting against viral infection, although the GPR146-mediated protection is eliminated by IRF3/HES1-signalling, which suggests a potential therapeutic significance of both GPR146 and HES1 signalling in viral infection.

Acknowledgements

This work was supported by National Natural Science Foundation of China [31570896, 81672811 and 81272369]; Joint Research Institute for Science and Society (JoRISS) [14JORISS01]; Doctoral Fund of Ministry of Education of China [20130076110013]; Science and Technology Commission of Shanghai Municipality [15JC1401500].

Authors contributions

BD, MQ, MYL and HJH conceived and designed the experiments. HJH, NZ, QQX, RYC, CFZ, NW and LW performed the experiments. HJH, HR and BD analysed the data. HJH and BD wrote the paper and HJH and NZ contributed equally to this work.

Disclosures

We declare that we have no conflict of interest.

References

1 Isaacs A, Lindenmann J. Virus interference. I. The interferon. *Proc R Soc Lond B Biol Sci* 1957; **147**:258–67.
2 Sadler AJ, Williams BR. Interferon-inducible antiviral effectors. *Nat Rev Immunol* 2008; **8**:559–68.
3 Hertzog P, Forster S, Samarajiwa S. Systems biology of interferon responses. *J Interferon Cytokine Res* 2011; **31**:5–11.
4 Alvarez-Curto E, Milligan G. Metabolism meets immunity: the role of free fatty acid receptors in the immune system. *Biochem Pharmacol* 2016; **114**:3–13.
5 Zhang Z, Wang Z, Ren H, Yue M, Huang K, Gu H *et al.* P2Y(6) agonist uridine 5'-diphosphate promotes host defense against bacterial infection via monocyte chemoattractant protein-1-mediated monocytes/macrophages recruitment. *J Immunol* 2011; **186**:5376–87.
6 Ohta A. A metabolic immune checkpoint: adenosine in tumor microenvironment. *Front Immunol* 2016; **7**:109.
7 Hu J, Oda SK, Shotts K, Donovan EE, Strauch P, Pujanauski LM *et al.* Lysophosphatidic acid receptor 5 inhibits B cell antigen receptor signaling and antibody response. *J Immunol* 2014; **193**:85–95.
8 Yan Y, Jiang W, Liu L, Wang X, Ding C, Tian Z *et al.* Dopamine controls systemic inflammation through inhibition of NLRP3 inflammasome. *Cell* 2015; **160**:62–73.
9 Guo C, Xie S, Chi Z, Zhang J, Liu Y, Zhang L *et al.* Bile acids control inflammation and metabolic disorder through Inhibition of NLRP3 Inflammasome. *Immunity* 2016; **45**:802–16.
10 Gloriam DE, Schioth HB, Fredriksson R. Nine new human Rhodopsin family G-protein coupled receptors: identification, sequence characterisation and evolutionary relationship. *Biochim Biophys Acta* 2005; **1722**:235–46.
11 Yosten GL, Kolar GR, Redlinger LJ, Samson WK. Evidence for an interaction between proinsulin C-peptide and GPR146. *J Endocrinol* 2013; **218**:B1–8.
12 Kolar GR, Grote SM, Yosten GL. Targeting orphan G protein-coupled receptors for the treatment of diabetes and its complications: C-peptide and GPR146. *J Intern Med* 2017; **281**:25–40.
13 Li D, Qiu Z, Shao Y, Chen Y, Guan Y, Liu M *et al.* Heritable gene targeting in the mouse and rat using a CRISPR-Cas system. *Nat Biotechnol* 2013; **31**:681–3.
14 Wu Y, Quan Y, Liu Y, Liu K, Li H, Jiang Z *et al.* Hyperglycaemia inhibits REG3A expression to exacerbate TLR3-mediated skin inflammation in diabetes. *Nat Commun* 2016; **7**:13393.
15 Li R, Tan B, Yan Y, Ma X, Zhang N, Zhang Z *et al.* Extracellular UDP and P2Y6 function as a danger signal to protect mice from vesicular stomatitis virus infection through an increase in IFN-beta production. *J Immunol* 2014; **193**:4515–26.
16 Alatery A, Basta S. An efficient culture method for generating large quantities of mature mouse splenic macrophages. *J Immunol Methods* 2008; **338**:47–57.
17 Zheng Q, Hou J, Zhou Y, Yang Y, Xie B, Cao X. Siglec1 suppresses antiviral innate immune response by inducing TBK1 degradation via the ubiquitin ligase TRIM27. *Cell Res* 2015; **25**:1121–36.
18 Ross DA, Rao PK, Kadesch T. Dual roles for the Notch target gene Hes-1 in the differentiation of 3T3-L1 preadipocytes. *Mol Cell Biol* 2004; **24**:3505–13.
19 Yanguez E, Garcia-Culebras A, Frau A, Llompart C, Knobeloch KP, Gutierrez-Erlandsson S *et al.* ISG15 regulates peritoneal macrophages functionality against viral infection. *PLoS Pathog* 2013; **9**:e1003632.
20 Van der Beek MT, Claas EC, van der Blij-de Brouwer CS, Morfin F, Rusman LG, Kroes AC *et al.* Rapid susceptibility testing for herpes simplex virus type 1 using real-time PCR. *J Clin Virol* 2013; **56**:19–24.
21 McNab F, Mayer-Barber K, Sher A, Wack A, O'Garra A. Type I interferons in infectious disease. *Nat Rev Immunol* 2015; **15**:87–103.
22 Matsumoto M, Oshiumi H, Seya T. Antiviral responses induced by the TLR3 pathway. *Rev Med Virol* 2011; **21**:67–77.
23 Matsumoto M, Seya T. TLR3: interferon induction by double-stranded RNA including poly(I:C). *Adv Drug Deliv Rev* 2008; **60**:805–12.
24 Wu J, Chen ZJ. Innate immune sensing and signaling of cytosolic nucleic acids. *Annu Rev Immunol* 2014; **32**:461–88.
25 Wang Q, Liu X, Cui Y, Tang Y, Chen W, Li S *et al.* The E3 ubiquitin ligase AMFR and INSIG1 bridge the activation of TBK1 kinase by modifying the adaptor STING. *Immunity* 2014; **41**:919–33.
26 Fitzgerald KA, McWhirter SM, Faia KL, Rowe DC, Latz E, Golenbock DT *et al.* IKKε and TBK1 are essential components of the IRF3 signaling pathway. *Nat Immunol* 2003; **4**:491–6.
27 Honda K, Taniguchi T. IRFs: master regulators of signalling by Toll-like receptors and cytosolic pattern-recognition receptors. *Nat Rev Immunol* 2006; **6**:644–58.
28 Chow EK, Castrillo A, Shahangian A, Pei L, O'Connell RM, Modlin RL *et al.* A role for IRF3-dependent RXRα repression in hepatotoxicity associated with viral infections. *J Exp Med* 2006; **203**:2589–602.
29 Shang Y, Coppo M, He T, Ning F, Yu L, Kang L *et al.* The transcriptional repressor Hes1 attenuates inflammation by regulating transcription elongation. *Nat Immunol* 2016; **17**:930–7.
30 Watanabe T, Kawakami E, Shoemaker JE, Lopes TJ, Matsuoka Y, Tomita Y *et al.* Influenza virus–host interactome screen as a platform for antiviral drug development. *Cell Host Microbe* 2014; **16**:795–805.
31 George SR, O'Dowd BF, Lee SP. G-protein-coupled receptor oligomerization and its potential for drug discovery. *Nat Rev Drug Discov* 2002; **1**:808–20.
32 Sodhi A, Montaner S, Gutkind JS. Viral hijacking of G-protein-coupled-receptor signalling networks. *Nat Rev Mol Cell Biol* 2004; **5**:998–1012.
33 Kawai T, Akira S. The role of pattern-recognition receptors in innate immunity: update on Toll-like receptors. *Nat Immunol* 2010; **11**:373–84.
34 Takeuchi O, Akira S. Pattern recognition receptors and inflammation. *Cell* 2010; **140**:805–20.
35 Sato M, Suemori H, Hata N, Asagiri M, Ogasawara K, Nakao K *et al.* Distinct and essential roles of transcription factors IRF-3 and IRF-7 in response to viruses for IFN-α/β gene induction. *Immunity* 2000; **13**:539–48.
36 Wathelet MG, Lin CH, Parekh BS, Ronco LV, Howley PM, Maniatis T. Virus infection induces the assembly of coordinately activated transcription factors on the IFN-β enhancer *in vivo*. *Mol Cell* 1998; **1**:507–18.
37 Randall RE, Goodbourn S. Interferons and viruses: an interplay between induction, signalling, antiviral responses and virus countermeasures. *J Gen Virol* 2008; **89**:1–47.
38 Rong H, Shen H, Xu Y, Yang H. Notch signalling suppresses regulatory T-cell function in murine experimental autoimmune uveitis. *Immunology* 2016; **149**:447–59.
39 Rani A, Greenlaw R, Smith RA, Galustian C. HES1 in immunity and cancer. *Cytokine Growth Factor Rev* 2016; **30**:113–7.

Supporting Information

Additional Supporting Information may be found in the online version of this article:

Figure S1. (a) The potential STAT1- and HES1-binding sites in the promoter of human *GPR146* were predicted by ALGGEN-PROMO. (b) Sequences of CRISPR target sites for mouse *Gpr146* in the genome. (c) The Cas9 endonuclease-mediated genome editing led to a deletion of 148 bases. (d) Results from primers used for the identification of mutations in (c) by PCR amplification. (e) Quantitative PCR analysis of *Gpr146* expression in PEMs from $Gpr146^{+/+}$ and $Gpr146^{-/-}$ mice. (f) Quantitative PCR analysis of *Tlr3* expression in PEMs from $Tlr3^{+/+}$ and $Tlr3^{-/-}$ mice. (g) Quantitative PCR analysis of *Gpr146* expression in $Tlr3^{+/+}$ and $Tlr3^{-/-}$ PEMs stimulated with Poly (I:C) (10 μg/ml) and LPS (500 ng/ml) for 4 hr. *Gapdh* was used as an internal control for quantitative PCR. The data are shown as the mean ± SD. $***P < 0{\cdot}001$; ns, not significant. All experiments were performed two or three times with similar results.

Table S1. The primer sequences for quantitative PCR analysis.

